Article ID: 6326(1999)03 - 0593 - 06

Effect of trace Sc and Zr on aging behavior and tensile properties of 2618 alloy①

Yu Kun(余 琨), Li Songrui(李松瑞), Li Wenxian(黎文献), Xiao Yude(肖于德)
Department of Materials Science and Engineering
Central South University of Technology, Changsha 410083 P. R. China

Abstract: The aging behavior of 2618 (Al-Cu-Mg-Fe-Ni) alloy added trace Sc and Zr was studied by Vicker's hardness measurement at 200 and 300 ℃, and the tensile properties(yield strength, ultimate tensile strength and elongation) of alloys were measured at 20, 200, 250 and 300 ℃. The microstructures were observed by using optical microscope, SEM and TEM. It was found that the addition of Sc and Zr to 2618 alloy resulted in a uniform distribution of fine coherent $Al_3(Sc,Zr)$ precipitates which had obvious aging hardening effect and made the S' phase precipitate more homogeneously. The strength of alloy increased at ambient and elevated temperature without a decrease of ductility because of the precipitation strengthening and thermal stability of $Al_3(Sc,Zr)$ particles. The ductile fracture of alloy occurred by microviod nucleation, growth and coalescence, so the microvoid coalescence was the dominant fracture mechanism. $Al_3(Sc,Zr)$ particles could inhabit the recrystallization process of alloy 2618.

Key words: scandium; zirconium; addition; 2618 alloy; tensile property **Document code: A**

1 INTRODUCTION

The aluminum and aluminum alloys added trace scandium have great improvement in mechanical properties, thermal stability, weldbility etc[1]. Scandium is considered to be a hopeful trace element to develop advanced wrought aluminum alloy due to a dispersed phase Al_3Sc precipitating in Al-base alloy[2]. The previous investigators[3,4] showed the phase Al_3Sc with a $Ll_2(AuCu_3)$ structure is fine coherent with the matrix and has great precipitation hardening effect. The previous studies of aging behavior mainly concentrated on the Al-Sc binary system[3] and Al-Mg-Sc alloy[4~5], but the research reports about the influence of Sc on typical precipitation hardening alloy Al-Cu-Mg system have hardly been seen. And Yelagin[6] found that another trace element zirconium in Al-Sc alloy was contribute to forming a ternary phase $Al_3(Sc, Zr)$ which has better effects on alloy's aging hardening. So, this work is based on the confirmation of the strengthening potential of Sc and the nature of $Al_3(Sc,Zr)$ precipitate, then added trace Sc and Zr in 2618 (Al-Cu-Mg-Fe-Ni) alloy and intended to develop a wrought aluminum alloy which have higher mechanical properties, especially thermal strength than that of 2618 alloy and discussed the influence of Sc and Zr on the microstructure of alloy.

2 EXPERIMENTAL METHODS

Compositions (mass fraction, %) of alloys used in this investigation are listed in Table 1.

Table 1 Chemical compositions of the alloys used in this study

Alloy NO.	Cu	Mg	Fe	Ni	Sc	Zr	Al
A(2618)	2.21	1.20	0.98	1.08	—	—	Bal.
B	2.23	1.21	0.93	1.09	0.3	0.3	Bal.

The ingots of alloys were homogenized at 500 ℃ for 10 h, then hot-rolled at 450 ℃ from 16 mm to 7 mm, and finally cold-rolled into sheets of 2 mm thickness. After solution treated in salt bath at 510 ~ 515 ℃ for 30 min and

① Received Oct.10, 1998; accepted Jan.27, 1999

quenched into room-temperature water, the specimens were immediately aged at 200 and 300 ℃ respectively. The hardness measurements were made at room temperature on the aged specimens immediately after artificial aging by using HVA-10A Vicker's hardness tester. The specimens for tensile test were aged at 200 ℃ for about 16 ~ 20 h according to the peak of aging hardness curves. Tensile tests were performed on an Instron 8032 tensile machine with computerized data acquisition. The ductility was measured as engineering strain to failure (percentage elongation) equal to $\Delta L/L_0$, where L_0 is initial length. The tensile specimens for high temperature test were held at the elevated temperatures for 15 min, then tensed at the rate 1 mm/min. Microstructures of alloy were observed by using Nephoto-2 optical microscope, H-800 transmission electron microscope and KYKY-1000B scanning electron microscope. Thin foil for TEM observations were obtained by jet electropolishing in a solution of 25 % nitric acid and 75 % methyl alcohol at - 15 ~ - 25 ℃.

3 RESULTS AND DISCUSSION

3.1 Aging hardness measurement

Fig.1 shows the variation of hardness of both alloy A and B as a function of aging time at 200 and 300 ℃ respectively.

At 200 ℃, the hardness values of alloy B increase more quickly than that of alloy A. The bright-field micrograph of alloy B (Fig.2(a)) shows some double-layer particles which have an average size about 20 ~ 30 nm existing in as-quenched condition. The morphology of deformation contrast region of the particle shows that such phase is coherent with the matrix. Because such phase can remain coherent with the matrix at 200 ℃ for a long time (Fig.2(d)), and it only exist in the alloy B with a composition that Sc: Zr > 0.5, it should be $Al_3(Sc,Zr)$ phase in a Al-Cu-Mg based alloy[3~6]. In order to produce a fully coherence, the $Al_3(Sc,Zr)$ phase and the matrix must be strained by equal and opposite force. The lattice mismatch δ between $Al_3(Sc,Zr)$ and Al is about 1.6 %. As a result, a high coherent strain energy exists in the matrix around the $Al_3(Sc,Zr)$ particles and it is difficult for the dislocations move through this strain fields. Therefore the hardness of alloy B is higher than that of alloy A.

Another factor for the high hardness of alloy B is that the coherent strain fields are preferential sites for S' phase, which is a useful strengthening phase in the alloy, to nucleate. It can be proved by Fig.2(b), a few needle shape phases has formed after aging 5 h in alloy B. Those are S' phase in Al-Cu-Mg alloy[8]. But according to the normal sequence of S phase precipitate: SSS (super-saturated solid solution) → GPB (Guinier-Preston-Bagaryatskii zone) → S' (metastable phase) → S, it hardly forms S'

Fig.1 Hardness-time curves of aged alloy A and B at different temperatures
(a) —200 ℃; (b) —300 ℃

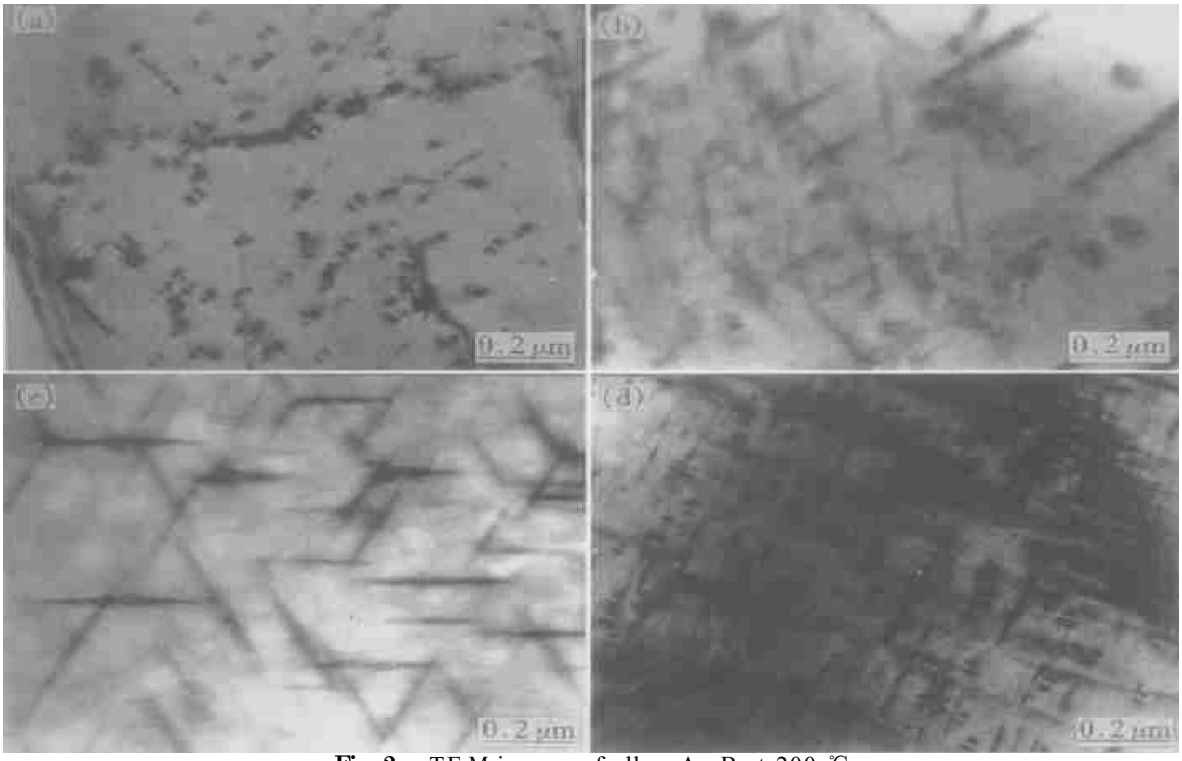

Fig .2 TEM images of alloy A, B at 200 ℃
(a) —Alloy B in as-quenched condition; (b) —Alloy B aged 5 h;
(c) —Alloy A aged 20 h; (d) —Alloy B aged 20 h

phase in Al-Cu-Mg alloy aged 5 h[7]. Therefor, it can get to the conclusion that $Al_3(Sc,Zr)$ particles may accelerate the precipitate of *S'* phase.

The peak hardness value of alloy B is 125 Hv and about 25 Hv higher than that of alloy A. Based on the aging curves and TEM observation, it can be deduced $Al_3(Sc,Zr)$ particles have additional aging hardening effect at this period. In one hand, $Al_3(Sc,Zr)$ is a potent strengthener in Al-base systems. On the other hand, $Al_3(Sc,Zr)$ particles are very effective in stabilizing substructures, thus allowing the *S'* phase to precipitate more homogeneously. It can be seen in Figs.2(c) and (d) the *S'* phase in alloy B is more dispersed than that in alloy A. Hence, the peak hardness of Alloy B is higher than that of alloy A.

The aging temperature has a great effect on the hardness variation of alloys. The hardening curves at different temperature show that the alloy achieves peak hardness quickly and the value is lower at higher temperature. It is a common behavior in most aging aluminum alloy.

3.2 Tensile properties and fractography

The tensile properties for alloy A and B at 20, 200, 250 and 300 ℃ are shown in Fig.3. It will be noted that the yield strength and ultimate strength of alloy B increase about 60 ~ 80 MPa at room temperature and 30 ~ 40 MPa at 300 ℃. But the ductility changes slightly. It means that $Al_3(Sc,Zr)$ particles introduces a high strength with high ductility to the Al-Cu-Mg alloy. This phenomenon is also observed in some Al-Mg alloys[5~8].

The fractography of tensile specimens at room temperature and 300 ℃ show the fracture of alloy belongs to ductile fracture. The microvoid coalescence is the dominant fracture mechanism in alloy A and B at both ambient and elevated temperatures, as illustrated in Fig.4. During void coalescence, sheets of small void

Fig.3 Tensile properties of alloys at different temperature
(a) —Yield strength, 0.2%; (b) —Ultimate strength; (c) —Elongation

nucleate, grow and coalesce from dispersed particles to form void sheets in strain-localized regions. Intrinsic resistance to microvoid fracture increases with temperature for IM aluminum alloys. Elevated temperature affects this increase by promoting stress relaxation around second-phase particles and enhances recovery at particle/matrix interfaces. So the ductility of alloy at elevated temperature increases obviously.

3.3 Microstructures of alloy

Figs.5 and 6 are the optical micrographs of alloy A and B in cold-rolled condition and as-quenching condition. Alloy A has been recrystallized after quenching. There are some insoluble second phases, which always are Al_xFeNi phase in Al-Cu-Mg-Fe-Ni system[9]. But the recrystallization phenomenon in alloy B is not as obvious as in alloy A. Through TEM observation of as-quenched alloy B (Fig.7(a)), it can be known that $Al_3(Sc,Zr)$ particles pin subgrain and grain boundaries during recrystallization process.

It is well known that both the coarse constituent particles and the fine dispersoids can have an effect on the recrystallization process[11]. Coarse particles (diameter $d>1\ \mu m$), such as Al_xFeNi phase in the Al-Cu-Mg-Fe-Ni alloy, can act as preferential sites for nucleation of recrystallization due to the increased strain of the matrix around these particles that occurs during rolling. The disperoids inhibit recrystallization by pinning subgrain boundaries and preventing recrystallization. The pinning force of the dispersoid on the boundary per unit area, F/A, can be expressed as

$$F/A = 3fV_b/2r$$

Where V_b is the boundary energy, f is the volume fraction and r is the average size of the dispersions[11]. So, the $Al_3(Sc,Zr)$ particles with small radii (10~20 nm, a high f/r ratio) will provide a large retarding force on migrating boundaries and impede the recrystallization process. Based upon this microstructural examination, the $Al_3(Sc,Zr)$ particles is very effective in stabilizing substructure, thus allowing the use of strain-hardening and grain boundary strengthening to enhance the strength of alloy B besides the precipitate strengthening of S' and $Al_3(Sc,Zr)$ phase. The subgrain coalescence nucleation mechanism is involved in the recrystallization process (Fig.7(b)). elevated temperatures, as illustrated in Fig.4. During void coalescence, sheets of small void

4 CONCLUSIONS

(1) The aging hardening of 2618 (Al-Cu-Mg-Fe-Ni) alloy added trace Sc and Zr is

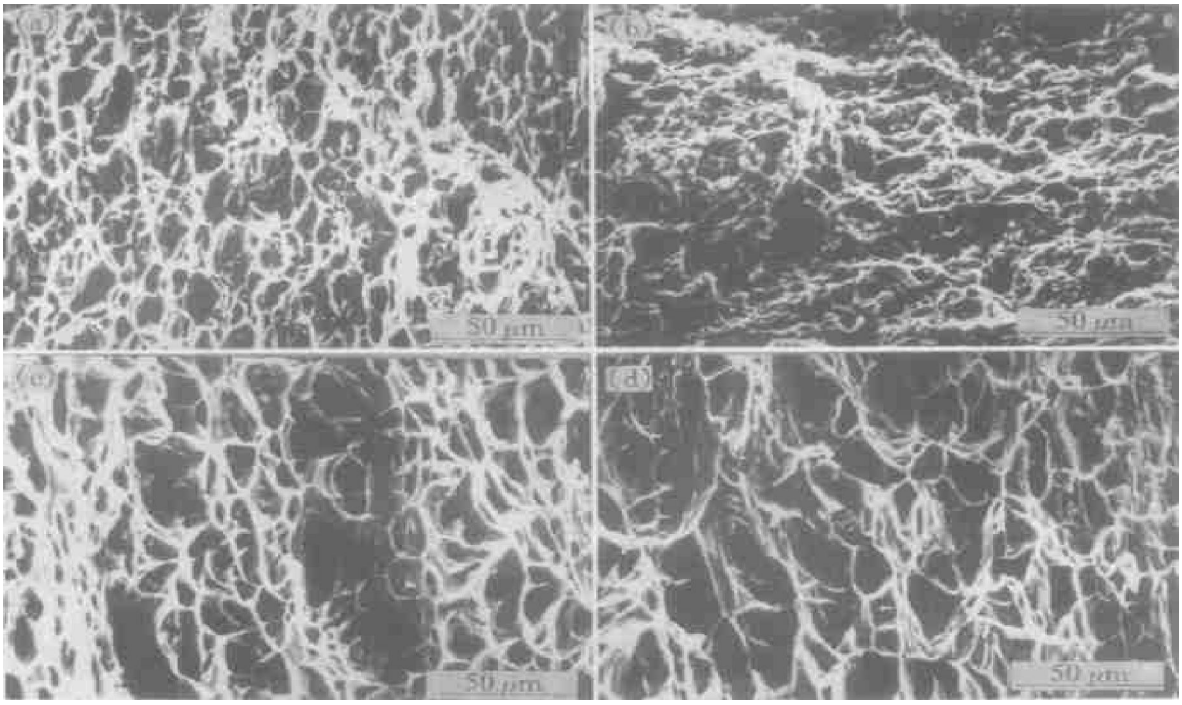

Fig .4 The fractography of tensile samples A, B at different temperature
(a) —A, 20 ℃; (b) —B, 20 ℃; (c) —A, 300 ℃; (d) —B, 300 ℃

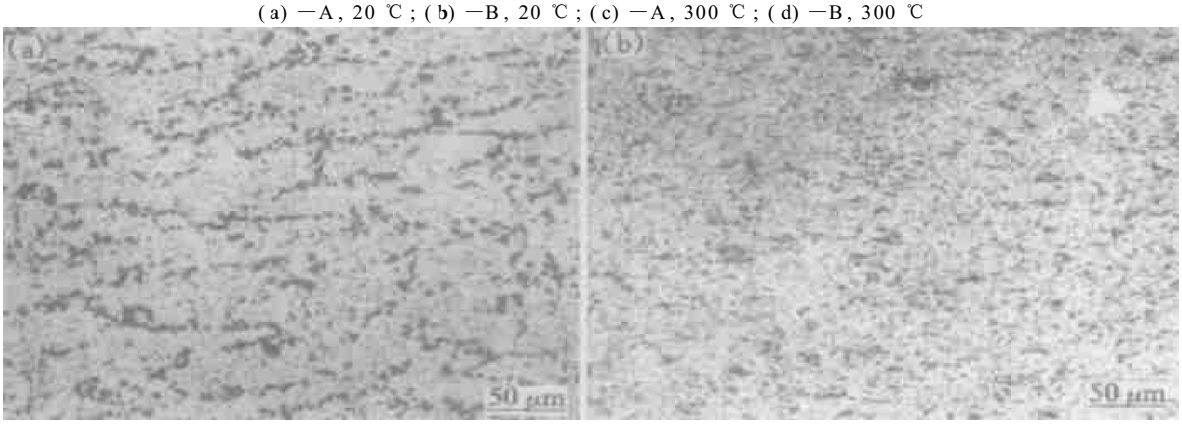

Fig .5 Optical micrographs of alloy A and B in cold-rolled condition
(a) —Alloy A; (b) —Alloy B

obvious. Vicker's hardness increase 20 ~ 30 Hv at 200 and 300 ℃ respectively.

(2) The dispersed Al_3(Sc, Zr) particles make the *S'* phase precipitate more homogeneously, so the tensile strength of alloy increase both at ambient and elevated temperature. Furthermore, the ductility of alloy changed slightly because of the good character of Al_3(Sc, Zr) phase. The microvoid coalescence is the dominant fracture mechanism in the test alloys.

(3) Al_3(Sc, Zr) particles can inhabit the recrystallization process of 2618 alloy in as-quenched condition because they can pin subgrain and grain boundaries.

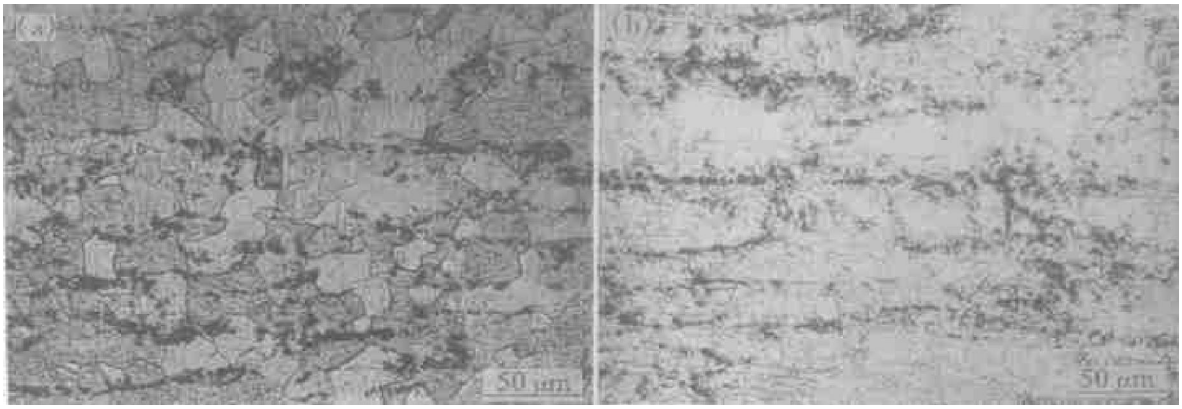

Fig.6 Optical micrographs of alloy A and B in as-quenched condition
(a) —Alloy A; (b) —Alloy B

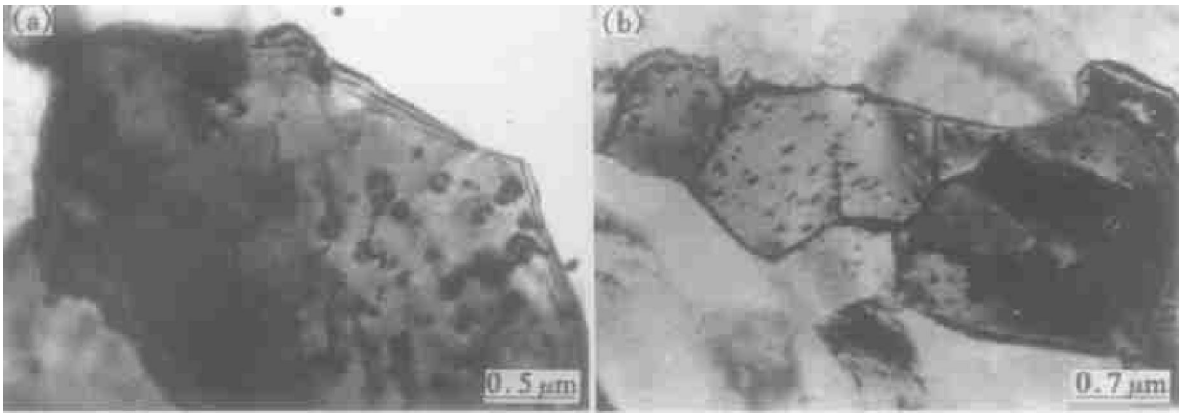

Fig.7 TEM micrograph of alloy B in as-quenched condition

REFERENCES

1 Ling Zhaoqi. Material Reviews (in Chinese), 1992, (3): 10.
2 Елагин В И, Ахаров В В and Xie Xiekui, Light Metals, (in Chinese), 1993, (3): 54.
3 Blake N and Hopkins M A. J Mater Sci, 1985, 20: 2861.
4 Hyung-Ho Jo, Shin-Itiroh Fujikawa. Mater Sci Eng, 1993, A171: 151.
5 Ralph R S and Craig L J. Metall Mater Trans A, 1990, 21A: 421.
6 Yelagin V I and Zakharov V. Phys Met Metall, 1985, 60(3): 88.
7 David A P and Kenneth E E. Oxford: Phase Transformations in Metals and Alloys. Alden Press, 1981.
8 Shin Hancheng and Ho New-jin. Metall Mater Trans A, 1996, 27A: 2479.
9 Bergsma S C and Li X. J Mater Eng & Perform, 1996, 5(1): 100.
10 Hyland R W. Metall Trans A, 1992, 23A: 1947.
11 Gorelik S. Recrystallization in Metals and Alloys. Moscow: MIR Publishers, 1981.
12 Yin Zhimin, Gao Yongzheng and Pan Qinglin. The Chinese Journal of Nonferrous Metals, (in Chinese), 1997, 7(4): 75.

(Edited by Zhu Zhongguo)